01 Oct 2006

Adaptive Critic Neural Network Force Controller for Atomic Force Microscope-Based Nanomanipulation

Qinmin Yang

Jagannathan Sarangapani
Missouri University of Science and Technology, sarangap@mst.edu

Recommended Citation

Q. Yang and J. Sarangapani, "Adaptive Critic Neural Network Force Controller for Atomic Force Microscope-Based Nanomanipulation," *Proceedings of the 2006 IEEE International Symposium on Intelligent Control (2006, Munich, Germany)*, pp. 464-469, Institute of Electrical and Electronics Engineers (IEEE), Oct 2006.
The definitive version is available at https://doi.org/10.1109/CACSD-CCA-ISIC.2006.4776690

Proceedings of the 2006 IEEE
International Symposium on Intelligent Control
Munich, Germany, October 4-6, 2006

Adaptive Critic Neural Network Force Controller for Atomic Force Microscope-based Nanomanipulation

Qinmin Yang and S. Jagannathan

***Abstract*—Automating the task of nanomanipulation is extremely important since it is tedious for humans. This paper proposes an atomic force microscope (AFM) based force controller to push nano particles on the substrates. A block phase correlation-based algorithm is embedded into the controller for the compensation of the thermal drift which is considered as the main external uncertainty during nanomanipulation. Then, the interactive forces and dynamics between the tip and the particle, particle and the substrate are modeled and analyzed. Further, an adaptive critic NN controller based on adaptive dynamic programming algorithm is designed and the task of pushing nano particles is demonstrated. This adaptive critic NN position/force controller utilizes a single NN in order to approximate the cost functional and subsequently the optimal control input is calculated. Finally, the convergence of the states, NN weight estimates and force errors are shown.**

I. Introduction

The nanomanipulation research aims at manipulating and handling nanometer size objects with nanometer precision [1-10,12-13]. It has become a recent topic [9] because it is also the first and fundamental step for achieving a complex functional nano device. Some nanotechnology applications can be found in fields like biotechnologies and life science (DNA, molecules and protein study), data storage (hard drive design) or material science (carbon nanotube or surface film characterization).

However, for industrial scale manufacture of commercial nanotechnology products, nanomanipulation of particles, which requires an interdisciplinary approach, must overcome several challenges. At present, assembly of small nano structures using available nano-manipulation techniques typically consist of ten to twenty particles and may take an experienced user a whole day to construct using Atomic Force Microscope (AFM) as the manipulator and under tightly controlled environmental conditions. To efficiently accomplish such tasks or even more complex ones, the manipulation process should be automated in order to minimize human intervention.

It is highly desirable to manipulate the particles in ambient conditions. In ambient conditions, nanomanipulation encounters multiple external disturbances, which are nonlinear and can result in major problems. Among these uncertainties, thermal drift is the most important one. Research presented in [13] provides a satisfactory real-time drift compensation algorithm, based on which, controllers can be designed without considering the influence of the thermal drift.

At the same time, the experimental samples used in nanomanipulation can be fragile. Applying an inapropriate force could damage nano objects and the AFM tip. Thus, designing controllers for the manipulation and handling of nano scale objects poses a much greater challenge in terms of accommodating the system nonlinearities and uncertainties. In fact, a near optimal control of AFM tip is necessary in order to apply suitable force to accommodate the fragile samples while ensuring that the system nonlinearities are compensated.

There has been a great deal of effort to realize the near optimal control for nonlinear systems, which involves the solution of HJB (Hamilton-Jacobi-Bellman) equation [2]. Recently, Murray et al. [2] proposed an adaptive dynamic programming (ADP) scheme to obtain a near optimal controller for affine nonlinear systems. In this paper, we apply this idea of HJB equation and set up the practical method for obtaining the nearly optimal control of continuous-time nonlinear systems using neural networks. We use successive approximation techniques in the least-squares sense to solve the HJB equation. A two layer NN is tuned offline to approximate the cost function. The trained NN is utilized to calculate the optimal/near optimal control input for nanomanipulation. Using [2], the convergence of the NN weights, tracking and force errors are shown.

II. Interaction Forces

In our work, the nano particles are first pretreated and then distributed on the substrate, which then will be manipulated by the AFM tip. The AFM tip apex is assumed to be a spherical ball with radius R_t = 30 nm, while the particle radius is denoted as R_p, β is the pushing angle, which is the angle between the pushing direction and the horizontal plane. Interactive forces among the AFM tip, particle, and substrate after the tip contacts the particle can be described by Fig. 1. Here A_{ps} denotes adhesion forces between particle and substrate, F_{ps} and F_{tp} represent the particle-substrate and tip-particle attractive/repulsive interaction forces, while f_{ps} and f_{tp} correspond to the

The authors are with the Electrical and Computer Engineering Department, University of Missouri-Rolla, Rolla, MO 65401 USA (e-mail: qyy74@ umr.edu). Research supported in part by NSF #0296191 and Intelligent Systems Center.

frictional forces for the particle-substrate and tip-particle respectively. Elastic deformation between the particle and the substrate is considered. The indentation is denoted as d .

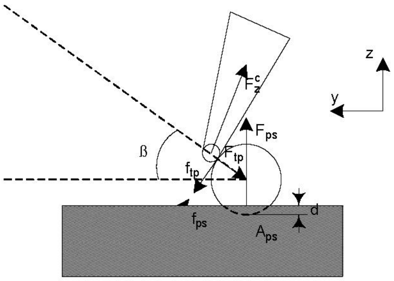

Fig. 1. The interacting forces between AFM tip, nanoparticle and substrate.

Gravitational forces are relatively small in the nano scale and, therefore, are neglected. The main components of the adhesion forces are van der Waals, capillary, and electrostatic forces [1]. Therefore, the adhesion force between particle and substrate is given by $A_{ps} = A_{ps}^{vdw} + A_{ps}^{cap} + A_{ps}^{es}$. The analysis of these contact and the frictional forces is very important for nano manipulation modeling.

A. Van der Waals Forces

The van der Waals force is caused by a momentary dipole moment between atoms. Depending upon the object geometry and the material type, van der Waals force between atoms or molecules is proportional to the inverse of the sixth power of distance between the molecules [3] as

$$A_{ps}^{vdw} = \frac{2HR_p^3}{3h^2(h+2R_p)^2} \qquad (2.1)$$

where H is Hamaker constant, and h is the particle-substrate distance.

Since we are interested in the manipulation task carried out in an ambient environment, there will be a liquid layer on the surface of the sample. Therefore, $H = \sqrt{(H_{tip} - H_{liquid})(H_{particle} - H_{liquid})}$ [4]. Also considering the surface roughness, van der Waals forces become [5]

$$A_{ps}^{vdw} = \frac{2HR_p^3}{3h^2(h+2R_p)^2}\left(\frac{h}{h+b/2}\right)^2 \qquad (2.2)$$

where b is the peak to peak height of the surface irregularity.

B. Capillary Forces

Due to the presence of the water layer on the surface of the particle and the substrate, a liquid bridge is formed between them at close contact as shown in Fig. 2.

In [6], molecular dynamic simulations have shown that the macroscopic capillarity theory should hold down to radius of curvature of the order of some molecular size. By assuming that (i) r << p << Rp, (ii) the surfaces are coated with a film of constant thickness e, (iii) the contact angle is zero, and (iv) the surfaces attraction through the liquid phase is negligible, the capillary force can be written as [7]

$$A_{ps}^{cap} = 4\pi\gamma R_p(1 - \frac{h-2e}{2r}) \qquad (2.3)$$

where γ is the liquid (water) surface energy, e is the thickness of the water layer, and r is the radius of curvature of the meniscus as shown in Fig. 2.

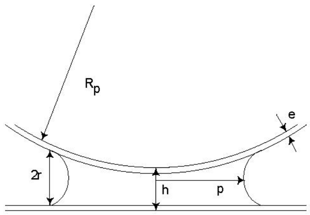

Fig. 2. Capillary force parameters during a sphere and flat surface contact.

C. Electrostatic Forces

In the case of non-conducting particles, there are charges trapped around the perimeter of the particles, and during pushing or contact, tribo-electrification process introduces local charges. For general cases, a model for the electrostatic forces is desirable. However, by grounding a (semi) conducting substrate such as Si, Au, or HOPG, the electrostatic forces can be greatly reduced [1]. Moreover, the nonconductive particles can be coated with Au, and all the substrate and particles can be grounded. We are using gold particle in our experiments, and it was reported that the electrostatic forces A_{ps}^{es} is less than one percent of the capillary force and therefore ignored [8].

D. Frictional Forces

During pushing, the friction between the particle-substrate and the particle-tip also play an important role. Similar to the case of macro domain, as the particle is sliding smoothly on the substrate, the frictional force at the micro/nano scale can be simply given as

$$f_{ps} = \mu_{ps} F_{ps} \qquad (2.4)$$

where μ_{ps} is the particle–substrate sliding friction coefficient. Also, frictional force between the tip and particle needs to be taken into account.

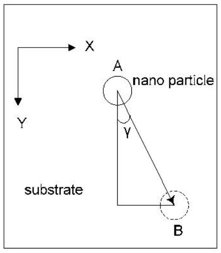

Fig. 3. Coordinate frames of the 2-D AFM image.

III. DYNAMIC MODEL

The micro-physics of the nanomanipulation has to be considered [7, 8] when manipulating objects in the nano domain. Modeling with all of the forces mentioned above is necessary for pushing nano-spheres laying on a planar substrate. The objects considered in this work include nano-particles of diameter 30 to 500 nm, which is required to be pushed from point A to B, as shown in Fig. 3. The angle between y axis and the pushing direction is denoted as γ.

A. Elastic Deformation of the Particle

Since the contact area between the particle and AFM tip is very small, only the vertical deformation between the particle and substrate will be considered [1]. The JKR (Johnson-Kendall-Roberts) model analysis is employed [10] here and the indentation of the particle is given as

$$\begin{aligned} a^3 &= R_p \cdot (F_{ps} + 3\pi R_p w + \sqrt{6\pi R_p w F_{ps} + (3\pi R_p w)^2}) / K \\ d &= a^2 / R_p - \frac{2}{3}\sqrt{3\pi w a / K} \end{aligned} \tag{3.1}$$

where a is the contact radius and d is the indentation.

B. Interacting Force Analysis

The interacting forces occurring between the tip, particle, and substrate are shown in Fig. 1. Since the tip is very small compared to the diameter of the particle, the AFM cantilever can be seen as a point object at the apex of the tip. A point mass model of the forces during pushing is derived in [1].

Let us assume that the surface of the substrate is ideally smooth in order to arrive at the dynamics. After the particle is detached from the substrate, assume that the particle is pushed at a constant low speed in a way of purely sliding as

$$\begin{aligned} &F_{tp} \sin\beta + A_{ps} + f_{tp} \cos\beta = F_{ps}, F_{tp} \cos\beta = f_{tp} \sin\beta + f_{ps} \\ &f_{ps} = \mu_{ps} F_{ps}, f_{tp} \cdot R_p = f_{ps} \cdot (R_p - d) \end{aligned} \tag{3.2}$$

and

$$\begin{aligned} F_{ps} &= \frac{A_{ps} \cos\beta}{\cos\beta - (1 - d / R_p + \sin\beta)\mu_{ps}} \\ F_{tp} &= \frac{(1 - d / R_p)\sin\beta + 1}{\cos\beta} \mu_{ps} F_{ps} \end{aligned} \tag{3.3}$$

Treating the AFM tip as a cantilever, denote the deflections of the probe along the x, y and z axes as ζ_x, ζ_y and ζ_z. In AFM-based manipulation systems, only ζ_z can be measured, which satisfies the following

$$m_c^* \ddot{\zeta}_z + b_z \dot{\zeta}_z + k_z \zeta_z = F_z^c + F_y^c k_z / k_{yz} \zeta_z \approx F_z^c \tag{3.4}$$

$$F_z^c = f_{tp} \cos\phi + F_{tp} \sin\phi \tag{3.5}$$

where $\phi = \beta - \alpha$, and α is the cantilever tilt angle from the base guaranteeing the point contact of the particle with the substrate. The terms k_z and b_z represent the elastic and damping coefficients of the cantilever along the z axes respectively, m_c^* is the cantilever effective mass and $b_z = 2\pi f_r m_c^* / Q_c$, where f_r is the cantilever resonance frequency and Q_c is the quality factor in air. Equation (3.4) shows that ζ_z can be seen as a measure of the force F_z^c applied on the particle.

Additionally, for atomic resolution positioning, piezoelectric actuators are utilized to move the stage in AFM systems. By denoting the sample position on the stage as x_s, y_s, z_s for each direction respectively, the dynamics of the stage are given as [1]

$$\begin{aligned} &\frac{1}{w_x^2}\ddot{x}_s + \frac{1}{w_x Q_x}\dot{x}_s + x_s = \tau_x - F_x = \tau_x - f_{ps}\cos\gamma \\ &\frac{1}{w_y^2}\ddot{y}_s + \frac{1}{w_y Q_y}\dot{y}_s + y_s = \tau_y - F_y = \tau_y - f_{ps}\sin\gamma \\ &\frac{1}{w_z^2}\ddot{z}_s + \frac{1}{w_z Q_z}\dot{z}_s + z_s = \tau_z - F_{ps} + A_{ps} \end{aligned} \tag{3.6}$$

where w is the resonant frequency, Q is the amplification factor and τ is the stage driving forces.

IV. DRIFT COMPENSATION IMPLEMENTATION

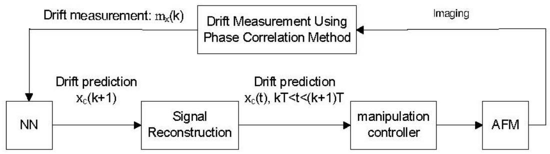

Fig. 4. Block diagram of the proposed drift compensator.

Due to thermal changes in ambient conditions, drift, normally called thermal drift, usually appears in successive AFM scans of a sample even when the scanning parameters are not altered. In the *x-y* plane, drift can be observed as a translation between different images, which depends on thermal changes and other unclear factors. From the height information of the sample, drift can be noticed even in the *z* direction. The drift velocities on the *x-y* plane are reported to vary from 0.01~0.1 nm/s [12]. So the drift between two images taken at 256 sec interval can be as much as 25.6 nm, which is comparable to the diameter of the particles that are normally manipulated. In our experiments, drift in the *z*-direction is about 0.005nm/s [13], which is considered negligible. Due to unexpected thermal drift, the nano-manipulation task can fail unless compensated.

Our first goal is to develop a drift compensation scheme to estimate and compensate the drift in the *x* and *y* directions so that nanomanipulation can be performed as if drift does not exist. Fortunately, experiments show that the drift in *x* and *y* directions can be seen as a translational movement, not rotation [12]. In addition, there is negligible correlation between the two. The block diagram of the proposed compensation system is depicted in Fig. 4. For simplicity, only the drift in the *x* direction is shown [13]. Due to the working principles of AFM, the sample topographic information is not available during the pushing procedure. So that the solution is stated as follows: 1) the sample is scanned at a constant frequency; 2) at each iteration, after obtaining the scanning data, the drift, $x_c(t)$ and $y_c(t)$, is estimated and predicted; 3) during the subsequent time interval before the next scanning, the pushing task can be performed via drift compensation.

In the proposed scheme, the drift is measured by using a block phase correlation algorithm at each sampling time. Based on current and previous data, drift for the subsequent sampling instant can be predicted. Further, signal reconstruction technique is applied to obtain a drift function in continuous time, which is directly applicable to controller design. For more details, refer to [13]. Consequently, the controller can be designed as if the drift does not exist.

First, define the system states as $s=\begin{bmatrix}x_s & y_s & z_s & \dot{x}_s & \dot{y}_s & \dot{z}_s\end{bmatrix}^T$. In order to accommodate the effects of drift, the system states will change to $s_r = s + s_c$ where s_r is the position of the particle on the stage coordinates, and $s_c=\begin{bmatrix}x_c & y_c & z_c & \dot{x}_c & \dot{y}_c & \dot{z}_c\end{bmatrix}^T$ is the drift value at the current time instant. The amount of drift in the *x-y* plane, x_c, y_c, can be estimated satisfactorily by using our drift compensator scheme from [13], while z_c is negligible. Therefore, the compensator development can be easily combined into the controller by adjusting the desired system trajectories as $s_d=\begin{bmatrix}x_d+x_c & y_d+y_c & z_d & \dot{x}_d+\dot{x}_c & \dot{y}_d+\dot{y}_c & \dot{z}_d\end{bmatrix}^T$. In other words, the relative position of the particle with respect to the stage can be calculated and thus be controlled to track the desired trajectory.

V. CONTROLLER DESIGN

After compensating the influence of the drift, our goal is to design a control input that guarantees a desired stage motion and applied force on the cantilever with a minimum cost. In this section, first assume there is no drift.

From (3.6), the nanomanipulation process can be simply written in affine form as

$$\dot{s} = f(s) + g(s)\cdot u \tag{5.1}$$

where

$$g(s)=\begin{bmatrix}0 & 0 & 0\\ 0 & 0 & 0\\ 0 & 0 & 0\\ w_x^2 & 0 & 0\\ 0 & w_y^2 & 0\\ 0 & 0 & w_z^2\end{bmatrix} \tag{5.2}$$

known. The performance measure can be defined as

$$\begin{aligned}V &= \int_{t_0}^{\infty}[q(s(s_0,\tau))+u^T(s_0,\tau)r(s_0,\tau)u(s_0,\tau)]d\tau \\ &= \int_{t_0}^{\infty}[q(s(s_0,\tau))+u^T(s_0,\tau)ru(s_0,\tau)]d\tau\end{aligned} \tag{5.3}$$

Without loss of generality, by setting $t_0 = 0$, the cost function/control law pair takes the form of $(V(s_0,t_0),u(s_0,t_0)) = (V(s_0),u(s_0))$. Using this notation, the Hamilton-Jacobi-Bellman (HJB) equation is defined as

$$HJB(V,u)=\frac{dV(s)}{ds}(f(s)+g(s)u)+q(s)+u^Tru=0 \tag{5.4}$$

for the time-invariant case [2].

By differentiating HJB equation with respect to u, we can obtain the desired relationship between the optimal control law and the optimal cost functional value as

$$u=-\frac{1}{2}r^{-1}g^T(s)\left[\frac{dV(s)}{ds}\right]^T \tag{5.5}$$

Then a desired adaptive dynamic programming (ADP) learning algorithm is formulated as follows [2]:

1. Initialize the algorithm with a stabilizing cost function/control law pair $(V_0,\ u_0)$, with a positive definite Hessian at x = 0, $\frac{d^2V_0(0)}{dx^2}>0$.
2. For i = *0, 1, 2 ...* run the system with control law u_i, record the resultant state trajectories and corresponding cost functional values along the trajectories as $V_{i+1}(s)=\int_0^{\infty}(q(s)+u_i^Tru_i)dt$.
3. For i = *0, 1, 2, ...* let $u_{i+1}=-\frac{1}{2}r^{-1}b^T(s)[\frac{dV_{i+1}(s)}{ds}]^T$.
4. Go to Step 2 if performance is not reached.

Proof: Refer [2]. It is shown in [2] that, the sequence of the cost function/control law pairs exist, and the control law can stabilize the plant with the cost function becoming the Lyapunov function. And further, the cost functional sequence will converge to the optimal cost.

The proposed algorithm requires a two-layer NN to approximate the value function and the optimal control input is calculated using (5.5). However, to realize this algorithm for a system with unknown dynamics requires the full exploration of the state space in order to obtain the cost function, which will be an impossible feat. Thus, an alternative choice is to explore only local state space and implement an approximation technique.

According to [11], a two-layer NN can be used to approximate any nonlinear continuous function over the compact set when the input layer weights are selected at random and held constant whereas the output layer weights are only tuned provided sufficiently large number of nodes in the hidden-layer is chosen. Furthermore, due to the generalization capability of the trained network, one can update the approximation locally in a neighborhood of each trajectory without needing to explore the entire state space. Hence, $V(x)$ is approximated by using a NN, as

$$V_L(s)=W_1^T\sigma(W_2^Ts) \tag{5.6}$$

where the activation function vector $\sigma(x):\Omega\to\Re$, is continuous, $\sigma(0)=0$ and the NN weights are W_1, W_2. The weights will be tuned to minimize the residual error in a least-squares sense over a set of points within the stability region of the initial stabilizing control. Least squares solution attains the lowest possible residual error with respect to the NN weights.

Thus, our adaptive critic NN controller based on ADP algorithm can be stated as:

1. Define a neural network as $V_L(s)=W_1^T\sigma(W_2^Ts)$ to

approximate the smooth function of $V(x)$.

2. Select an initial admissible feedback control law u_1.
3. For *i* = *1, 2* ..., recording the system response and collecting $V^{(i)}$ associated with u_i. If $V^i(s_0)\leq\eta$, or $V^{i-1}(s_0)-V^i(s_0)\leq\varepsilon$, then the optimal cost function $V^*=V^{(i)}$ and the algorithm stops, where η, ε are pre-selected small positive constants. Otherwise, continue the algorithm and go to the next step.
4. Select a specified number of equally spaced states/cost function pairs to train a NN using least square method (LSM), which is designed to approximate $V^{(i)}(s)$.
5. Update the control as
$$u_{i+1}=-\frac{1}{2}r^{-1}g(s)^T\frac{\partial V^{(i)}(s)}{\partial s} \qquad (5.7)$$
where $\frac{\partial V^{(i)}(s)}{\partial s}$ is obtained from the output of the NN.
6. Go to step 3.

The architecture of the whole system including controller is shown in Fig. 5. The system is launched with an initial stable controller and begins to iterate until an acceptable near optimal controller is reached.

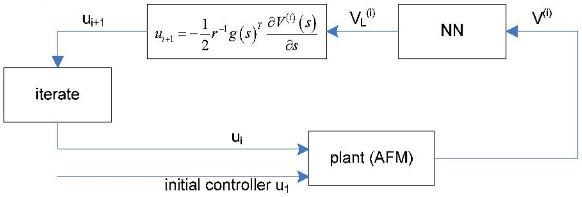

Fig. 5. Architecture of the whole system with ADP controller frame.

The optimal control law ensures that the system is stable which in turn guarantees that the states converge. However, this does not imply that the applied force is bounded. As stated above, improper applied force could damage the nano particles or even the AFM tip. The controller should guarantee that the force error is bounded. So following theorem presents that the applied force is also bounded when the optimal control input is applied to the stage for nanomanipulation.

Theorem 1: Assume that the desired position and its derivatives of the stage along with the desired force on the cantilever are bounded. Let the control input be provided by (5.5), then the force error is bounded.

Proof: Since the deflection of the cantilever on *z* direction is the direct measurement of the force, here we will only consider the boundedness of the deflection ζ_z. Indeed, its dynamics are given by (3.5). By combining (3.3) and (3.4), it can be rewritten as

$$m_c^*\ddot{\zeta}_z+b_z\dot{\zeta}_z+k_z\zeta_z=f_{tp}\cos\phi+F_{tp}\sin\phi \qquad (5.8)$$
$$=\frac{\cos\phi}{\cos\beta}(F_{ps}-A_{ps})+\sin\phi\cdot(1-\frac{\cos\phi\sin\beta}{\cos\beta})\frac{(1-d/R_p)\sin\beta+1}{\cos\beta}\mu_{ps}F_{ps}=h(s)$$

where

$$\begin{aligned}h(s)=A_{ps}\cdot&[(\cos\phi+\sin\phi(\cos\beta-\cos\phi\sin\beta))\ ((1-d/R_p)\sin\beta+1)\mu_{ps}\\&-(\cos\beta-(1-d/R_p+\sin\beta)\mu_{ps})\cos\phi]\\&/\cos\beta(\cos\beta-(1-d/R_p+\sin\beta)\mu_{ps})\end{aligned}$$

is a function of the states. By defining the force error as
$$\zeta_e=\zeta_z-\zeta_d \qquad (5.9)$$
equation (5.8) can be expressed as $m_c^*\ddot{\zeta}_e+b_z\dot{\zeta}_e+k_z\zeta_e=h(s)-k_z\zeta_d=h'(s)$, where ζ_d is the desired force, and $h'(s)$ is a continuous function of the states, which is also bounded. Further, since m_c^*, b_z, k_z are positive constants, it can be concluded that the force error is bounded or the actual force ζ_z, on the cantilever is bounded.

VI. Simulation Results

In this section, the NN based ADP will be implemented in order to push a nanoparticle from one place to the other. The initial state and the final goal of the nanomanipulation system for the task of pushing are given in Table 1.

TABLE 1: INITIAL AND FINAL STATE FOR PUSHING OPERATION

Item	Symbol	Unit	Desired value
position of the stage on *x*	x_S	nm	250
position of the stage on *y*	y_S	nm	433
deflection of the cantilever	ζ_z	nm	12.8

For our ADP-based NN implementation at each iteration the explored local state space is divided into 51 sampling points. At each point, a sample of the cost function is collected and then used for the network training.

Figs. 6 through 9 illustrate the performance of the adaptive critic NN controller based on adaptive dynamic programming algorithm. From a given initial point in the state space, the algorithm converged to a nearly optimal control strategy. The performance measure is chosen as

$$\begin{aligned}V&=\int_{t_0}^{\infty}[q(s)+u^Tru]d\tau\\&=\int_{t_0}^{\infty}\left[[x_e\quad y_e\quad \zeta_z]Q[x_e\quad y_e\quad \zeta_z]^T+u^Tru\right]d\tau\end{aligned}$$

where $Q=diag[1\quad 1\quad 1]$ and $r=diag[1\quad 1\quad 1]$ with x_e, y_e represents the position error between current and the desired one. The algorithm was initialized on the first iteration with a standard hybrid PD force controller, whose force response and control inputs are shown in Figs. 6 and 8 respectively. After the state reaches the desired position, the iteration count was incremented, and the NN approximation of the cost function was computed. Further, the control law was constructed and the system was restarted at the same initial state. The ADP-based NN controller performance is illustrated in Figs. 7 and 9. It can be seen that the control inputs generated by the control law (5.5) is indeed optimal compared to the initial stabilizing control. The algorithm was iterated eight times.

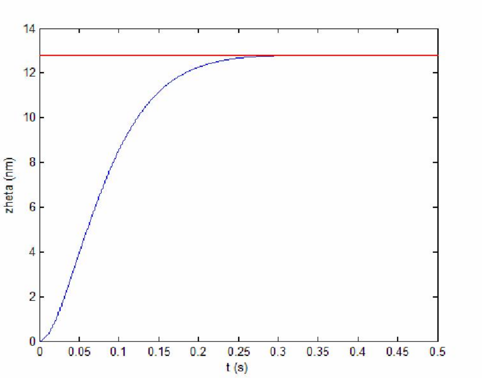

Fig. 6. PD controller performance (solid line – system force response; dashed line – desired force value).

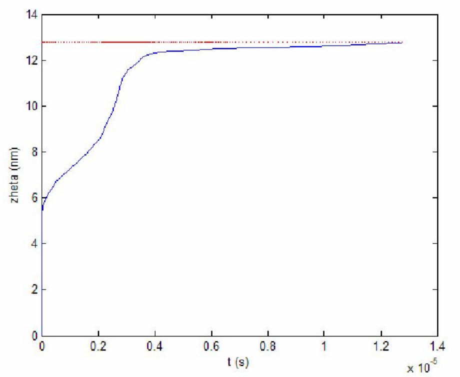

Fig. 7. Near optimal controller performance (solid line – system force response; dashed line – desired force value).

VII. CONCLUSIONS

The nano object manipulation is complex and requires a sophisticated controller to achieve an optimal performance. In this paper, an adaptive critic neural network controller based on adaptive dynamic programming is presented for guiding the stage so that the task of pushing a nano particle was realized. The embedded drift compensator in the controller is able to eliminate the influence of the drift. The simulation results demonstrate that the proposed controller is able to perform the pushing task successfully and ensures the boundedness of all the closed-loop signals.

REFERENCES

[1] M. Sitti and H. Hashimoto, "Controlled Pushing of Nanoparticles: Modeling and Experiments", IEEE/ASME Trans. on Mechatr, July 2000

[2] J. J. Murray, C. J. Cox, G. G. Lendaris, and R. Saeks, "Adaptive Dynamics Programming", IEEE Trans. on System, Man, and Cybernetics, vol. 32, no. 2, pp. 140-153, 2002.

[3] H.C. Hamaker, "The London-van der Waals Attraction Between Spherical Particles," Physica IV, No. 10, pp. 1058-1072, 1937.

[4] J. Israelachvili, "Intermolecular and Surface Forces," 2nd ed. London, U.K.: Academic, 1992.

[5] S. Saito, H. Miyazaki, and T. Sato, "Pick and place operation of a micro-object with high reliability and precision based on micro-physics under SEM," IEEE International Conference on Robotics and Automation, vol. 4, pp. 2736 – 2743, 1999.

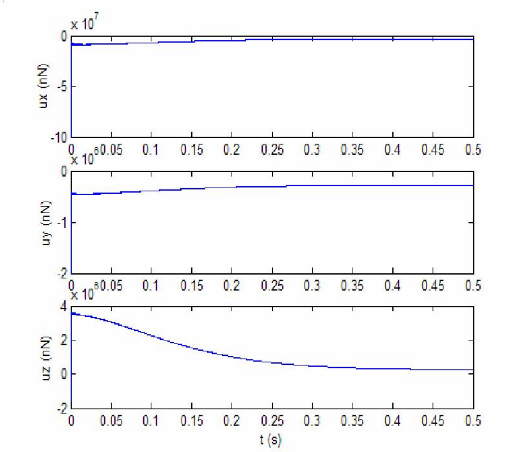

Fig. 8. Control inputs of the initial PD controller.

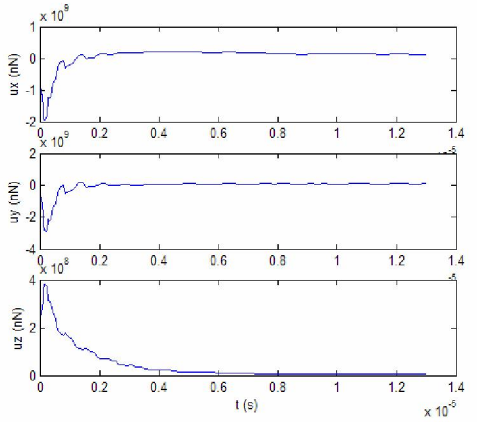

Fig. 9. Control inputs of the final near optimal controller.

[6] P. Thompson and M. Robbins, "Simulations of contact-line motion: slip and the dynamic contact angle," Phys. Rev. Lett. 63, 766, 1989.

[7] J. Crassous, E. Charlaix, H. Gayvallet, and J. Loubert, "Experimental study of a nanometric liquid bridge with a surface force apparatus," Langmuir, vol. 9, no. 8, pp. 1995–1998, 1993.

[8] F. Arai, D. Ando, and T. Fukuda, "Micro manipulation based on micro physics: Strategy based on attractive force reduction and stress measurement," in Proc. IEEE Int. Conf. Robotics and Automation, Pittsburgh, PA, pp. 236–241, 1995.

[9] M. Sitti, "Survey of nanomanipulation systems," Proc. of the IEEE Proceedings of the Nanotechnology, pp. 75 – 80, 2001.

[10] K. L. Johnson, and J. A. Greenwood, "An adhesion map for the contact of elastic spheres," J. Colloid. Interface Sci. 192, pp. 326-333, 1997.

[11] B. Igelnik, and Y. H. Pao, "Stochastic choice of basis functions in adaptive function approximation and the functional-link net," IEEE Trans. Neural Networks, Vol. 6, pp. 1320-1329, 1995.

[12] B. Mokaberi and A. A. G. Requicha, "Towards automatic nanomanipulation: drift compensation in scanning probe microscopes", IEEE Int. Conf. on Robotics and Automation, New Orleans, LA, April 25-30, 2004.

[13] Q. Yang, S. Jagannathan and E. W. Bohannan, "Block phase correlation-based automatic drift compensation for atomic force microscopes," Proc. of 5th IEEE Conf. on Nanotechnology, Nagoya, Japan, July 2005.